OIL DROPLET MANIPULATION USING LIQUID DIELECTROPHORESIS ON ELECTRET WITH SUPERLYOPHOBIC SURFACES

Tianzhun Wu[1], Yuji Suzuki[1], Nobuhide Kasagi[1] and Kimiaki Kashiwagi[2]
[1]The University of Tokyo, Japan
[2]Asahi Glass Co., Ltd, Japan

ABSTRACT

We propose a novel low-voltage droplet manipulation method "liquid dielectrophoresis on electret (L-DEPOE)" with superlyophobic surfaces (SLS), which enable high contact angle and low flow friction for water and oil. Charge stability of electret in liquid is much improved with new polymer coating, and SLS with electrodes are successfully fabricated, showing high mechanical robustness and extreme repellence for hexadecane droplets even with fast droplet motion. Low adhesion and contact angle hysteresis of SLS for oil droplets are experimentally demonstrated, indicating low motion resistance of droplet on SLS.

INTRODUCTION

Microfluidics has gained great success to miniaturize fluidic manipulation for biomedical and chemical applications such as µTAS. To aim at automation in a similar way with integrated chips (ICs) and simplify labor-intensive liquid handling process, droplet-based digital microfluidics now attract much interest. As the mainstream method for digital microfluidics, electrowetting on dielectrics (EWOD) can successfully generate, split, transport and merge aqueous droplets on planar surfaces [1]. However, EWOD is not directly applicable for non-aqueous or non-conductive liquids [2]. As an alternative, liquid dielectrophoresis (L-DEP) can be used to manipulate both water and oil [3-4], promising as the universal manipulation method for various droplet operations. However, L-DEP needs high voltage up to ~1 kV for oil [4] or AC frequency higher than 1 kHz for water [3], which restricts L-DEP from broader applications. We previously proposed a novel low-voltage droplet manipulation method named "L-DEP on electret (L-DEPOE)" by using polymer electret with quasi-permanent charges [5], and reduced the driving voltage to only 5 VDC for oil droplet transport [6].

It is recognized that high driving voltage required for EWOD and L-DEP roots from the dominant surface tension. Contact angle hysteresis (CAH) of a droplet becomes the major obstacle for contact line motion [7], especially for oil with low

surface tension γ (~24 mN/m) [8]. To reduce the flow resistance for droplet motion, low-wetting surfaces are necessary. Superhydrophobic surfaces repellent to water (γ~72 mN/m) have been combined with EWOD for this purpose [9], nevertheless they are not repellent to low-surface-tension liquid like oil [10]. On the other hand, superlyophobic surfaces (SLS) recently developed can achieve high contact angle (CA) and low CAH simultaneously for various liquids including water and oil [10-12]. We have clarified the design criteria and MEMS fabrication for high-performance SLS [12], and achieved extreme high static CA (θ_s=159˚) and low CAH $\Delta\theta$=8˚ for both water and oil. Based on these design rules, here we propose the combination of L-DEPOE with SLS to reduce droplet motion resistance. The prototype of L-DEPOE droplet manipulation with SLS is microfabricated and its performances are investigated.

CONFIGURATION AND PRINCIPLE

The basic configuration of L-DEPOE with SLS is schematically shown in Fig. 1. Compared with previous L-DEPOE devices [6], here the bottom flat surface is replaced by SLS with patterned conductive
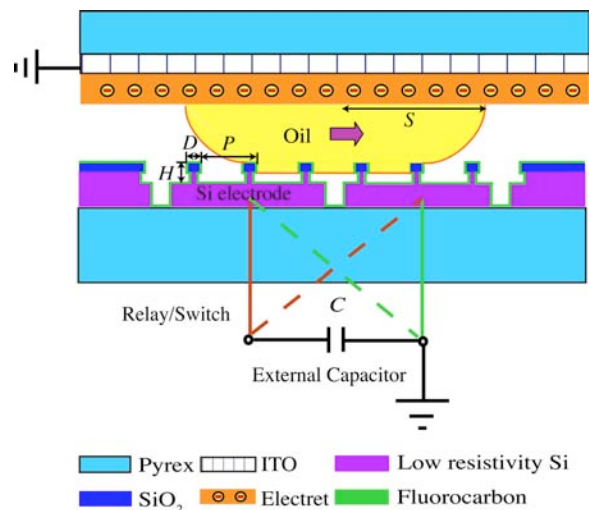

Figure 1. Schematic of droplet manipulation using L-DEPOE with SLS. An oil droplet can be switched between two Si electrodes when an external capacitor switches its connections between two electrodes by a relay/switch.

Si as embedded electrodes. A dielectric droplet such as oil can be moved between two electrodes under the non-uniform electrostatic field by the L-DEP force when an external capacitor switches its connection between two bottom electrodes using low-voltage electric relays or switches. The droplet has the intrinsic CA lower than 90˚ on the top flat electret surface, while has an apparent CA much larger than 90˚ on bottom SLS. By designing T-shape micro pillars with proper diameter D, pitch P and depth H, an oil droplet can be suspended with low contacting solid fraction f_s [12], and flow resistance due to solid-liquid interaction can be significantly reduced.

MATERIALS AND FABRICATIONS

Amorphous perfluoropolymer CYTOP® (CTL-809M, Asahi Glass Co., Ltd.) is chosen as electret due to its high surface charge density up to 1.5 mC/m^2 (~1200 V on 15 µm-thick film) and long-term charge stability (over 4000 hours in air) [5]. However, its charge stability is much reduced in liquid. As shown in Fig. 2a, surface voltage of 15 µm-thick CYTOP soaked in hexadecane decay quickly in only 3 hours, while with 5 µm-thick parylene overcoat it can survive for ~30 hours. By covering CYTOP with newly developed moisture-proof polymer, the electret charge stability can be much improved, and ~500 V is still available after 100 hours.

The electret substrate for liquid environment is fabricated by the procedures shown in Fig. 3. 200 nm-thick ITO is sputtered onto a 4-inch Pyrex wafer, and 3 µm-thick CYTOP is spin-coated and baked at 100˚C for 10 minutes and repeated for 5 times to obtain 15 µm-thick film, followed by 185˚C baking for 1.5 hours. Then, 5 µm-thick moisture-proof polymer is spin-coated as well as additional 100 nm-thick CYTOP layer to have hydrophobic surface on the electret. After that, the wafer is diced into 25 mm×25 mm samples and implanted charges by corona charging [5].
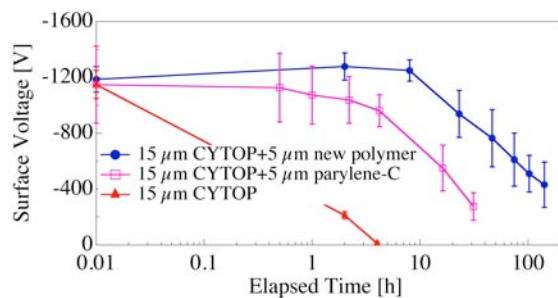
Figure 2. Charge decay of electrets in hexadecane. New moisture-proof polymer coating markedly improves the charge stability in liquid.
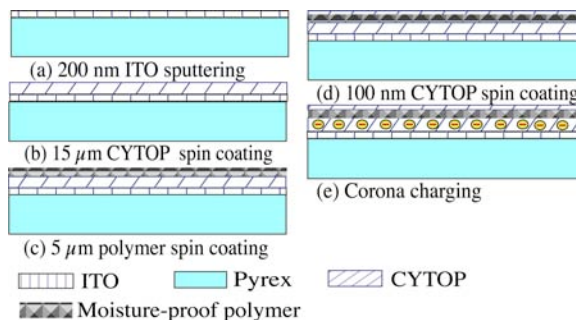
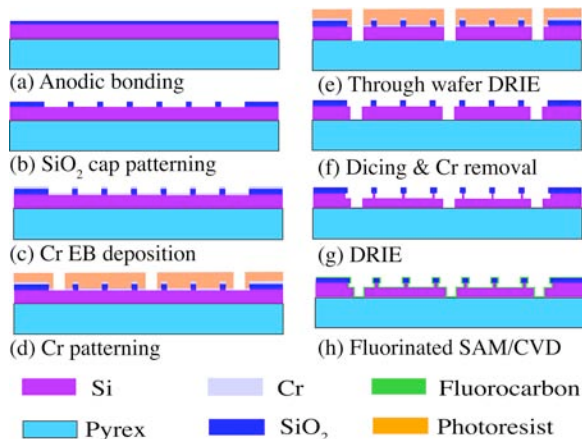*Figure 3. MEMS process of the electret substrate.*

Figure 4. MEMS process of SLS with patterned Si as embedded electrodes.

The fabrication process of SLS with patterned Si electrodes is shown in Fig. 4. A 4-inch Si wafer with a thickness of 100 µm is thermally oxidized to grow ~280 nm-thick SiO$_2$, and the oxide on one side is stripped by buffered HF. This is followed by anodic bonding with 525 µm-thick Pyrex (Fig. 4a). Then SiO$_2$ is patterned by standard photolithography and etched with CF$_4$ plasma to expose Si (Fig. 4b). To isolate Si electrodes, through-wafer deep reactive ion etching (DRIE) for 15 µm-width gap is employed with AZP4400 photoresist and 30 nm-thick Cr hard mask (Fig. 4c-e). After dicing and removing Cr (Fig. 4f), T-shape pillars are formed by DRIE (Fig. 4g) and finally fluorinated treatment for whole surfaces is made with chemical vapor deposition (CVD) of C$_x$F$_y$ using C$_4$F$_8$ plasma or self-assembled monolayer (SAM) in the vapor phase using PTFS (n-CF$_3$(CF$_2$)$_5$(CH$_2$)$_2$SiCl$_3$).

Figure 5 shows SEM images of fabricated SLS. Uniform etching profile with ~35 µm-depth and ~300 nm undercut for micro pillars (diameter D=4 µm) are successfully achieved by optimizing DRIE recipes (Figs. 5a-b), which leads to favorable mechanical and pressure robustness [12].

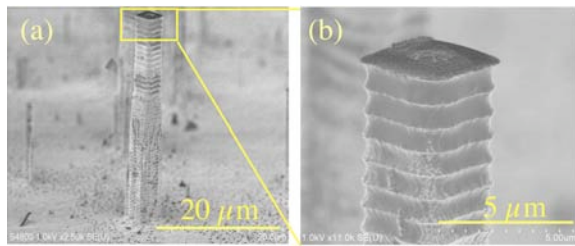We also compare the lyophobic performances of SLS by different surface functionlization methods of

Figure 5. SEM pictures for SLS fabrications. (a) cross-sectional view of ~35 μm-height T-shape pillars. (b) Magnification view of Fig. 5a. Undercut for the SiO₂ cap is only ~300 nm.

Figure 7. Static and Dynamic CAs of hexadecane on SLS with f_s=0.01. Dynamic CAs are measured when fixing the droplet by a syringe and move SLS slowly.
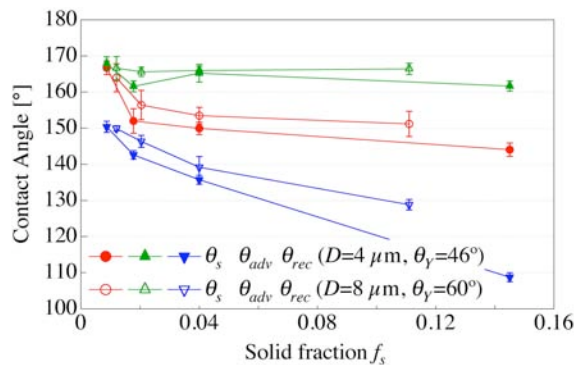

Figure 6. Comparison of hexadecane static and dynamic CAs on SLS with different functionlization methods by plasma CVD and SAM. Hexadecane intrinsic CA on C_xF_y by CVD is ~46° while for PFTS SAM it is ~60°.

C_xF_y and PFTS. As depicted in Fig. 6, due to higher intrinsic Young's CA θ_Y for PFTS, both static CA θ_s and advancing/receding CAs $\theta_{adv}/\theta_{rec}$ of SLS with PFTS treatment are higher than those with C_xF_y for various solid fraction. Hence, surface functionalization using PFTS is preferred for better SLS performance.

RESULTS AND DISCUSSIONS

As-fabricated SLS with embedded electrodes exhibit extreme low wetting performances for oil. Static CA θ_s=(167.1±2.0)° and $\Delta\theta$=(θ_{rec}-θ_{adv})~8° or CAH= ($\cos\theta_{rec}$-$\cos\theta_{adv}$)≈0.04 have been achieved for hexadecane on SLS (f_s=0.01) as shown in Fig. 7, which are best performances ever reported for hexadecane. Further experiments show the dynamic CAs are insensitive to droplet velocities, and only dependent on f_s. As shown in Fig. 8, advancing and receding CAs are almost unchanged for different droplet velocity on SLS with D=4 μm and P=10~40 μm (accordingly f_s ranges from 0.01 to 0.16, and only data for P=10 μm and P=40 μm are shown for clear visibility in Fig. 8), indicating applicability of SLS for fast droplet transport.

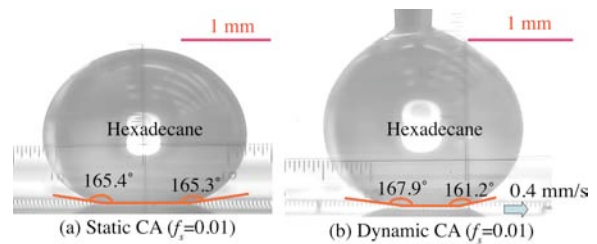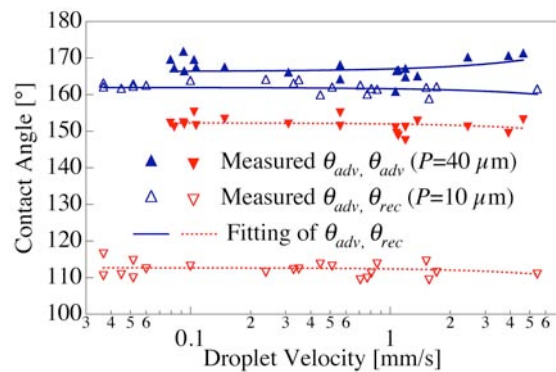It is also found that only when f_s is low enough

Figure 8. Dynamic CAs versus droplet velocities on SLS with different pitches (D=4μm, P=40 and 10 μm). Dynamic CAs are found insensitive to the droplet velocities

can SLS be favorable for low flow resistance. As shown in Fig. 9, a hexadecane droplet is sandwiched between a flat CYTOP surface (not yet charged) and SLS with two embedded electrodes, and then SLS substrate is moved in the horizontal direction. With f_s=0.021, SLS has lower CAH and weaker adhesion with the droplet, hence the droplet can easily slide on SLS but pin on the flat surface (Figs. 9a-c). When f_s=0.236, CAH and adhesion on SLS are even larger than those on the flat surface, leading to the pinning droplet on SLS (Figs. 9d-f). These facts can be explained by CAH force expressed as F_{CAH}= 2f_s•CAH•w, where w is the droplet contact line width perpendicular to the motion direction, and f_s•CAH is defined as *effective CAH*. For the flat CYTOP surface, f_s=1, and CAH=0.09, then effective CAH is 0.09. For SLS with f_s=0.021 and CAH=0.12, effective CAH yields 0.0025, which is smaller than 0.09. SLS with f_s=0.236 and CAH=0.56, yields effective CAH ~0.13>0.09. Further calculation indicates that the critical f_s yielding the same resistance with flat CYTOP surface is ~0.12.

By reducing effective CAH and hence hydrodynamic resistance using low-f_s SLS as the bottom substrate, the droplet velocity is expected to increase inside L-DEPOE microfluidics. We perform numerical simulation of the droplet motion driven by
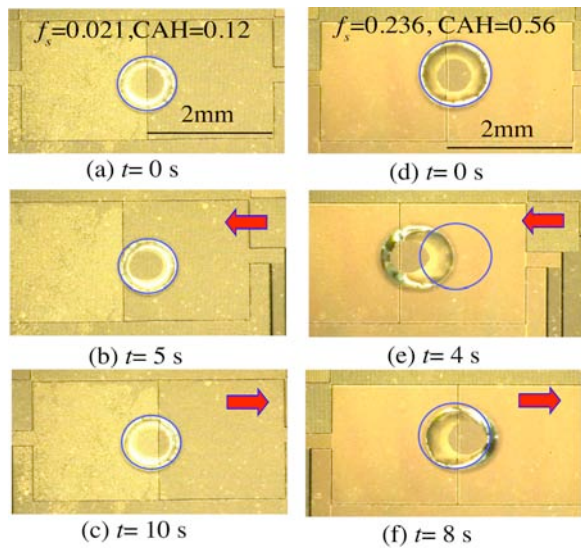
Figure 9. Top-view snap shots of a hexadecane droplet moving between the top flat CYTOP surface and the bottom SLS with 2 embedded electrodes (gap height ~300 µm). The SLS substrate is dragged in the horizontal direction. (a)~(c) for low f_s, droplet pins on the flat surface. (d)~(f) for high f_s, droplet pins on the SLS. The circle indicates the initial position of the droplet.
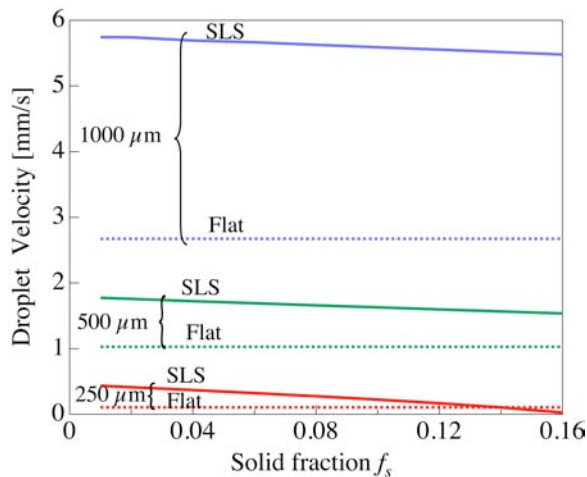

Figure 10. Simulation of droplet transport velocity driven by L-DEPOE with SLS for different f_s and S. A larger droplet benefits more from SLS, leading to faster motion.

L-DEPOE with SLS, following the similar modeling for L-DEPOE [8] while replacing CAH with effective CAH. The electret charge density is assumed 1.4 mC/m^2, and the external capacitance and the gap height are chosen 5 pF and 150 µm respectively. The dependences of droplet velocity with f_s and the hexadecane droplet feature radius S (see Fig. 1) are examined and shown in Fig. 10(the electrode size is assumed 2S). As shown in Fig. 10, when S=250 µm, the droplet velocity on SLS is slightly increased with reducing f_s, which is faster than the one on flat surface given f_s<0.14. When S increases to 500 µm

and 1000 µm, the velocities on both flat surface and SLS increase quickly to ~mm/s order, and the velocity is significantly higher on SLS than on flat surface. The fastest velocity reaches ~5.7 mm/s for S=1000 µm and f_s =0.01.

CONCLUSIONS

A novel low-voltage, low-friction oil droplet method integrating L-DEPOE and SLS has been proposed. Robust SLS with patterned Si as electrodes are fabricated and show high CA ~167° and low CAH Δθ~8° for hexadecane droplets. With the proposed SLS, reduced flow resistance for oil droplet motion is demonstrated, which significantly increases the droplet velocity.

ACKNOWLEDGEMENTS

REFENENCES

[1] S. Cho, H. Moon, and C. Kim, *J. Microelectro-mech. Syst.*, 12(1), pp. 70-80, 2003.

[2] D. Chatterjee, B. Hetayothin, A. Wheeler, D. King, and R. Garrell, *Lab Chip*, 6(2), pp. 199-206, 2006.

[3] S. Fan, T. Hsieh, and D. Lin, *Lab Chip*, 9(9), pp. 1236-1242, 2009.

[4] T. Jones, *Langmuir*, 18(11), pp. 4437-4443, 2002.

[5] Y. Sakane, Y. Suzuki, and N. Kasagi, *J. Micro-mech. Microeng.*, 18(10), 104011(1-6), 2008.

[6] T. Wu, Y. Suzuki, and N. Kasagi, *IEEE Int. Conf. MEMS'08*, Tucson, USA, 2008, pp. 591-594.

[7] H. Ren, R. Fair, M. Pollack, and E. Shaughnessy, *Sensor Actuat B-Chem.*, 87(1), pp. 201-206, 2002.

[8] T. Wu, Y. Suzuki, and N. Kasagi, *25th Japan Sensor Symp.*, Okinawa, Japan, 2008, pp. 785-786.

[9] J. Heikenfeld, and M. Dhindsa, *J. Adhes. Sci. Technol.*, 22 (3-4), pp. 319-334, 2008.

[10] A. Tuteja, W. Choi, M. Ma, J. Mabry, S. Mazzella, G. Rutledge, G. McKinley, and R. Cohen, *Science*, 318(5856), pp. 1618-1622, 2007.

[11] A. Ahuja, J. Taylor, V. Lifton, A. Sidorenko, T. Salamon, E. Lobaton, P. Kolodner, and T. Krupenkin, *Langmuir*, 24(1), pp. 9-14, 2008.

[12] T. Wu, Y. Suzuki, and N. Kasagi, *Int. Conf. µTAS'09*, Jeju, Korea, 2009, pp. 591-594.